

# Sensors for Force, Pressure, Distance, Angle, and Light Intensity

## Keywords:

Sensor, linearity, response time, measuring range, resolution, noise, strain gauge, piezoresistive effect, triangulation, HALL-effect, semiconductor, pn-junction.

## Measuring program:

Calibration of a force sensor and a pressure sensor, distance measurement with a laser distance sensor, measurement of the transmission ratio with an angle sensor, linearity of the output signal of a photo diode, measurement of the power of laser light, measurement of the velocity of a finger movement.

## References:

- /1/ NIEBUHR, J.; LINDNER, G.: „Physikalische Messtechnik mit Sensoren“, Oldenbourg-Industrieverlag, München
- /2/ SCHANZ, G. W.: „Sensoren“, Hüthig-Verlag, Heidelberg
- /3/ HAUS, J.: „Optical Sensors“, Wiley-VCH, Weinheim

## 1 Introduction

A sensor is a device for the quantitative acquisition of a physical or a chemical quantity. In most cases, the value  $w$  of the quantity is converted into an electrical voltage  $U$  or an electrical current  $I$ . By performing a *calibration*, the *calibration function*  $U(w)$  (or  $I(w)$  resp.) is obtained; it allows determining the value of the quantity from the measured value of the voltage or current. For calibrating a force sensor, for example, the sensor is submitted to varying, yet known forces  $F_i$  and the corresponding voltage  $U_i$  is measured in each case. Subsequently,  $U_i$  is plotted over  $F_i$  and a calibration curve is obtained by performing a fit on the measured values.

Important characteristic parameters of sensors are:

- *Linearity*: Often a linear relationship exists between the actual value of the quantity  $w$  and the output signal of the sensor, e.g. the voltage  $U$ . In this case:

$$U = k w + U_0$$

where  $k$  is the *calibration factor* and  $U_0$  the output voltage of the sensor for the case  $w = 0$ . In this case, the *calibration curve* is a *line*, the sensor operates in a *linear* manner. If  $U_0 = 0$ , a *proportionality* exists between  $U$  and  $w$ . This is the ideal case for a sensor.

- *Response time*: The response time is the time interval required for a change in the quantity  $w$  to cause a corresponding change in the output signal.
- *Measuring range*: The measuring range defines the range of values of the quantity  $w$ , which causes a change of the output signal which can be described by the calibration function, within a defined margin of error.
- *Resolution*: The resolution is the smallest change of the quantity  $w$ , which leads to a distinctively measurable change of the output signal.
- *Noise*: The inherent, random fluctuations in the output signal of a sensor are called noise. One of the main sources for the noise of many sensors is the electronics employed for the creation of the output signal.

The use of sensors in measurement technology, and industrial production has become widespread since it became possible to produce sensors in compact miniaturized packages, or even integrate them directly into IC's<sup>1</sup>. In this experiment, sensors for force, pressure in gases, distance, angle, and light intensity will be treated.

---

<sup>1</sup> IC: *Integrated Circuit*. An integrated electrical circuit inside a ceramic or plastic casing.

## 2 Theory

### 2.1 Bending Rod as a Force Sensor

The force sensors used in the introductory laboratory course transform a mechanical force of magnitude  $F$  into a voltage signal  $U$  that varies linearly with  $F$ .



Fig. 1: *Left:* Principle of force measurement using a bending rod (green) fixated on the left by a block (gray). The gravitational force  $\mathbf{F} = \mathbf{G}$  of a suspended weight (blue) causes a deformation of the staff which is measured by the strain gauge (SG, yellow). The mechanical limits (red) prevent overstraining the rod by excessive forces. *Right:* View into the casing of a force sensor used in this laboratory course. The strain gauges glued to the rod are very thin and barely visible. The cables are the connections of the SG. They run to the connecting terminal on the top left to which the measuring amplifier is connected.

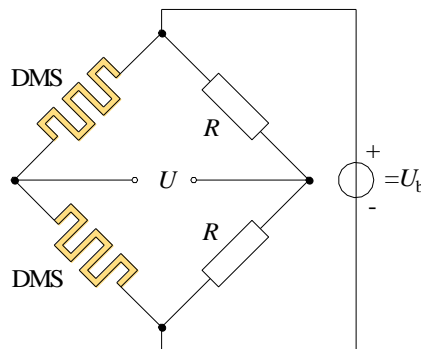


Fig. 2: Half bridge with two SGs of the same type and two equal resistors  $R$ . One SG is elongated while the other one is compressed.  $U_b$  is the supply voltage of the bridge,  $U$  the output voltage which is amplified by a measuring amplifier.

A bending rod (cf. Fig. 1) is used as the sensor. The staff is fixed at one end and elastically deformed by the force  $\mathbf{F}$ , HOOKE's law applies<sup>2</sup>. The rod is elongated on the top side while it is compressed on the bottom side. Elongation and compression are proportional to  $F = |\mathbf{F}|$ . The deformations are translated into changes in electrical resistance proportional to  $F$  by strain gauges (SG). The SGs are connected to form a *half-bridge* (cf. Fig. 2)<sup>3</sup>. The supply voltage  $U_b$  is connected to one bridge diagonal, while the output voltage  $U$  is measured at the other diagonal. Since this voltage is very small (in the mV range), it is amplified by a measuring amplifier which also provides the supply voltage  $U_b$ . The output voltage of the measuring amplifier,  $U_M$ , changes linearly with  $F$ .

### 2.2 Pressure Sensor on the Basis of the Piezoresistive Effect

A sensor of the type SENSORTECHNICS HCLA12X5DB is available for the measurement of pressure changes in gases. It is a semiconductor sensor and its operation is based on the *piezoresistive effect*, which is the change in electrical resistance of a material (in this case p-silicone, p-Si; cf. Chap. 2.5.1 for labeling) under the influence of mechanical tension. Fig. 3 (left) depicts the schematic setup for such a sensor. A silicone membrane with a width of several micrometers divides a gas-tight chamber in the centre, separating it into two gas-tight parts. The upper half of the chamber is connected (using a tube) to a volume of gas at pressure  $p_1$  while the other half is connected to a volume of gas having pressure  $p_2$ . A pressure difference  $\Delta p = p_2 - p_1$  causes the membrane to bulge towards the chamber with lower pressure. The border of the membrane is fitted with piezoresistive sensors that experience forces as a result of the defor-

<sup>2</sup> ROBERT HOOKE (1635 – 1703)

<sup>3</sup> Compare experiment „Measurement of Ohmic Resistances...“

mation of the membrane. The tension causes an elongation, and hence a change of resistance in the material<sup>4</sup> which is converted to a voltage signal by using a bridge circuit integrated in the sensor. The signal is amplified by an integrated circuit, which is also already part of the sensor. At the output of the pressure sensor, a voltage  $U$  is thus available which changes linearly with the pressure difference  $\Delta p$ .<sup>5</sup>

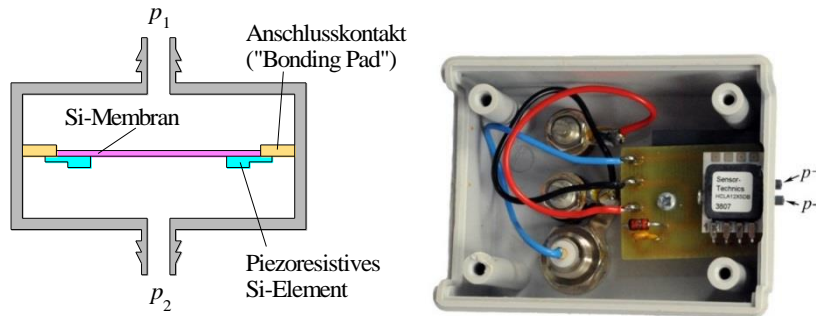


Fig. 3: *Left:* Schematic representation of a piezoresistive pressure sensor for measuring a pressure difference  $\Delta p = p_2 - p_1$ . *Right:* View into the casing of a pressure sensor used in this laboratory course. The sensor integrated in an IC can be seen on the right (inside) on a small circuit board. The tube connectors can be seen on the outside of the casing on the right ( $p_1 = p^-$ ,  $p_2 = p^+$ ).

### 2.3 Distance Sensor on the Basis of Triangulation

A laser distance sensor is used for distance measurements (type BAUMER OADM 12U6460/S35). The sensor uses the principle of triangulation (cf. Fig. 4 left). A thin, collimated beam of laser light from a laser diode is incident on the surface of an object O. The distance of the reflective surface to a plane of reference E within the sensor is to be measured. The centre of an objective L is placed at a lateral distance  $d$  from the exit of the laser beam. This objective focuses the light reflected at point C of the object onto a one dimensional CCD-array<sup>6</sup>. This results in a point image A at a distance  $q$  from the right border of the CCD-array. The distance  $q$  varies with the distance  $s$  between E and O. For the *triangle* ABC (hence the name *triangulation*) we have:

$$(1) \quad \tan \alpha = \frac{d + q}{s}$$

In addition, using the distance  $p$  between the central plane of the lens and the front side of the CCD-array (plane E) we get:

$$(2) \quad \tan \alpha = \frac{q}{p}$$

From this follows:

$$(3) \quad \frac{d + q}{s} = \frac{q}{p} \quad \rightarrow \quad s = \frac{(d + q) p}{q}$$

Provided that the device parameters  $d$  and  $p$  are known, the distance  $s$  may be determined by measuring the quantity  $q$ .

The signal of the CCD-array is captured by a microprocessor which determines the value of  $q$  from this data; together with the known geometrical data  $d$  and  $p$  the processor calculates the distance  $s$  and produces an output voltage signal  $U_{LDS}$  with a linear relationship to  $s$ . This signal is available at the sensor's output.

<sup>4</sup> The effect is comparable to the change of resistance of a metallic SG under elongation. The change in resistance associated with a certain elongation of a piezoresistive material is, however, significantly larger than in the case of a metallic SG. For metals,  $k = 2 - 4$ , for Si  $k \approx 100$  (cf. Experiment "Measuring ohmic resistances...").

<sup>5</sup> The electrical connection (bond) between the integrated circuit and the piezoresistive elements is established by thin bonding filaments connected to bonding pads.

<sup>6</sup> CCD: Charge Coupled Device. A one dimensional CCD-array consists of a number of e.g. 128 or 512 (or more) small photodetectors (pixels) with an individual width of a few micrometers arranged in a straight line.

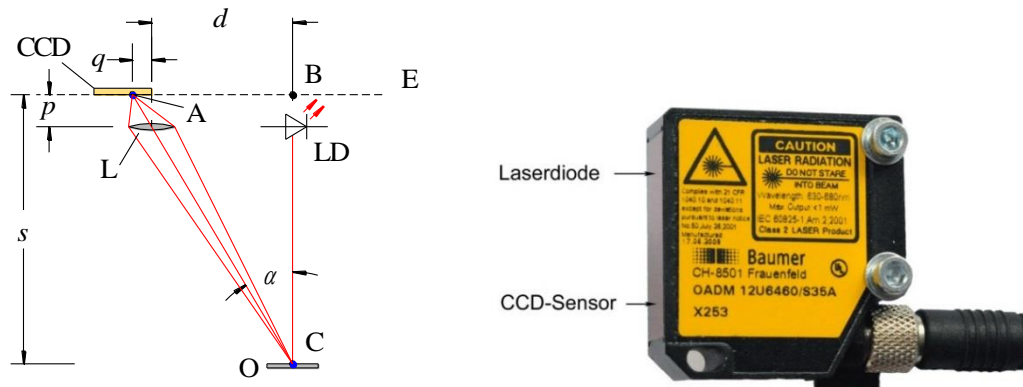


Fig. 4: *Left:* Operating principle of a laser distance sensor using triangulation (schematic). In reality, the objective L and the CCD-array may be skewed against the horizontal, in order to minimize distortions of the image of C within the measuring range of the sensor. *Right:* Photograph of the laser distance sensor used in the introductory laboratory course. The connecting cable for the supply voltage and the output signal is seen on the bottom right corner.

## 2.4 Angle Sensor on the Basis of the HALL-Effect

For the measurement of the angle of rotation about an axis, an angle sensor (type TWK-ELEKTRONIK PBA 12) based on the HALL<sup>7</sup>-effect will be used. We will only describe its basis here schematically. A detailed treatment of the Hall-effect is reserved for lectures in later semesters.

We consider a block of a suitable semiconductor material as depicted in Fig. 5 (grey), which is penetrated by a magnetic field  $\mathbf{B}$  (blue) oriented along the vertical direction, while an electric current  $I$  flows through it in the horizontal direction. In the microscopic view, the current is caused by the transport of positive and negative charge-carriers of charge  $\pm q$ , moving with the drift velocities  $\pm v$ . It is known from school, that moving charges in a magnetic field are subject to the LORENTZ<sup>8</sup> force  $\mathbf{F}$ , which is given by:

$$(4) \quad \mathbf{F} = q \mathbf{v} \times \mathbf{B}$$

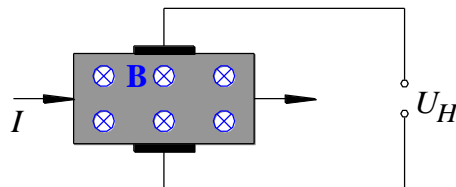


Fig. 5: Schematic representation of the Hall-effect. Refer to the text for labels.

In a setup according to Fig. 5, the LORENTZ force causes positive charge carriers to move to the top and negative charge carriers to the bottom. This results in a Hall-voltage  $U_H$  forming between the contacts (black) given by:

$$(5) \quad U_H \sim B$$

It is evident from Eq. (4), that the magnitude of the force  $\mathbf{F}$  depends on the angle  $\alpha$  between  $\mathbf{v}$  and  $\mathbf{B}$ . It holds:

$$(6) \quad F = q v B \sin \alpha = q v B_{\perp}$$

where  $B_{\perp}$  is the component of  $\mathbf{B}$  standing perpendicular on  $\mathbf{v}$ . A change of the force  $F$  is accompanied by a proportional change of the Hall-voltage. It holds:

$$(7) \quad U_H \sim B_{\perp}$$

<sup>7</sup> EDWIN H. HALL (1855 – 1938)

<sup>8</sup> HENDRIK A. LORENTZ (1853 – 1928)

Eq. (7) forms the basis for the angle sensor used in the experiment, its operating principle is depicted schematically in Fig. 6.

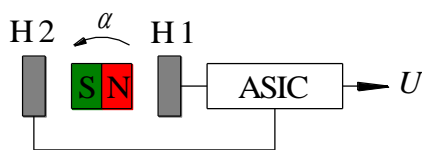


Fig. 6: Schematic of the angle sensor used in the experiment. Refer to the text for labels.

A small permanent magnet is mounted on the axis whose angular position  $\alpha$  is to be measured. Upon rotation of the axis, the magnetic field  $\mathbf{B}$ , caused by the magnet, is rotated by the same angle. This field penetrates two<sup>9</sup> Hall-sensors H1 and H2. Depending on the orientation of  $\mathbf{B}$ , H1 and H2 provide two different Hall-voltages, which are transformed by an ASIC<sup>10</sup> to create the output voltage  $U_w$  of the angle sensor, which is proportional to the angle  $\alpha$ .

## 2.5 Photodetectors

Photodetectors are used for the detection of light. Measurable quantities are the light power  $P_L$  with the unit W (Watt) or the light intensity  $I_L$  with the unit  $\text{W}/\text{m}^2$ . We will restrict ourselves from the multitude of different photodetectors to the photodiode. It converts the quantities  $P_L$  or  $I_L$  into an electric current  $I$  which changes in a linear fashion with  $P_L$ , or  $I_L$  respectively. A current to voltage converter may be used to convert the current  $I$  to a proportional voltage  $U$ , if the need arises.

Knowledge of solid state physics and semiconductor physics, which will be acquired in later semesters, is required for a detailed understanding of how a photodiode works. For this reason, we will restrict ourselves to a short description of the basics of its construction and operating principle.

### 2.5.1 Si-Semiconductor and pn Junction

The majority of photodiodes are manufactured from crystalline silicone (Si), which is a semiconductor. Every four valued atom in pure (*intrinsic*) Si is connected to four other Si atoms by covalent bonds (cf. Fig. 7). The four electrons of the outer shell are thus spatially fixated.

Doping of pure Si with five-valued atoms (*donors*) creates *n-silicon* (Fig. 8 left), which is a *n-semiconductor*<sup>11</sup>. Only four electrons are needed for the covalent bonds of the donor atom with the four neighboring Si atoms. The bond between the fifth electron (negative *n-charge carrier*) and the core of the donor atom is rather weak. This electron can thus move through the material nearly unobstructed.

By doping pure silicon with three-valued atoms (*acceptors*) *p-silicon* can be created (Fig. 8 right) which is a *p-semiconductor*. One electron is missing in the covalent bond of the acceptor atom with the four Si-

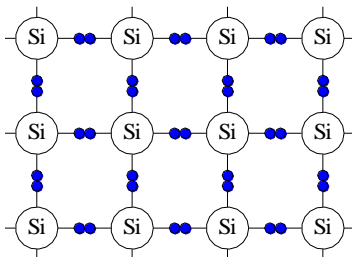


Fig. 7: Crystal structure of pure Si. The blue circles represent (schematically) the electrons making up the covalent bonds.

neighbors. This leaves a *hole*, which behaves like a positive charge carrier (*p-charge carrier*). This hole is able to capture an electron from its surrounding. The captured electron leaves a new hole, which can again capture an electron from its surrounding. The hole may thus move through the material, it is mobile.

<sup>9</sup> Two Hall-sensors are required in order to determine the sign of a rotation unambiguously.

<sup>10</sup> ASIC: Application Specific Integrated Circuit.

<sup>11</sup> The typical doping concentration in Silicone, which is used for the construction of photodiodes lies within the order of magnitude  $10^{15} - 10^{17}$  impurity atoms /  $\text{cm}^3$ . Pure Si contains approx.  $0.5 \times 10^{23}$  Si-atoms /  $\text{cm}^3$ .

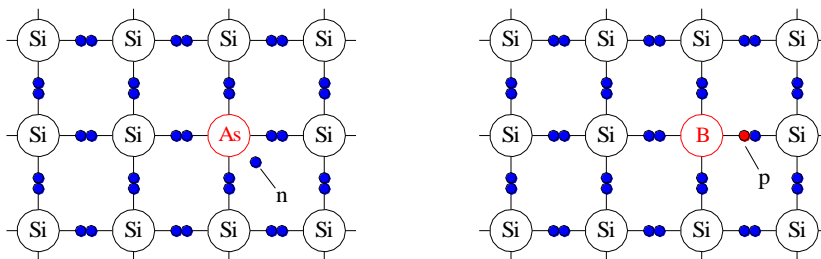


Fig. 8: *Left:* Crystal structure of n-Si where several four-valued Si-atoms are replaced by five-valued atoms, in this case arsenic (As). The fifth valence electron of the As atom is a mobile n-charge carrier. *Right:* Crystal Structure of p-Si where several four-valued Si atoms are replaced by three-valued atoms, in this case boron (B). The missing valence electron of the B atom, called a *hole*, is a mobile p-charge carrier.

When a p- and a n-semiconductor are brought into contact, a *pn junction* is formed (cf. Fig. 9). The concentrations of p- and n-charge carriers differ greatly in the contact region. This causes holes to diffuse from the p-Si to the n-Si where they recombine with the surplus electrons. Analogously, the surplus electrons from the n-Si diffuse into the p-Si region, recombining with the surplus holes. This causes the formation of a region without mobile charge carriers, hence called the *depletion zone* (*S*) or *barrier layer*. The diffusion process leaves positive ionized donors in the n side of the depletion zone and negative ionized acceptors on the p side (cf. Fig. 10). These ions are called *space charges*, they create an electrical field  $\mathbf{E}$  (*built-in-field*) in the depletion zone, also called *space charge region* in this context.

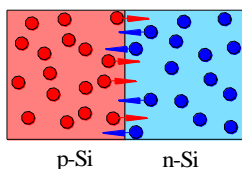


Fig. 9: Emergence of a pn junction by bringing two layers of p-Si and n-Si into contact. Diffusion of n-charge carriers (blue) to the p-Si and diffusion of p-charge carriers (red) to the n-Si occurs in the contact region.

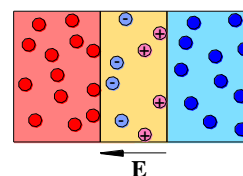


Fig. 10: Upon completion of the diffusion process of the p- and n-charge carriers, positive ionized donors  $\oplus$  are left in the n-layer, while negative ionized acceptors  $\ominus$  are left in the p-layer. A barrier layer *S* (yellow) results, in which the space charges generate an electrical field  $\mathbf{E}$ . The actual width ratios of the p-, n- and barrier layer differ considerably from this principle image.

## 2.5.2 Operating Principle of a Photodiode

We consider a photodiode on the basis of a pn junction (cf. Fig. 10). Irradiation of the photodiode with light causes absorption of photons. The energy of the photons is sufficient to create electron-hole pairs in the silicon through the *inner photoelectric effect*. This allows some electrons to make the transition from the valence band to the conduction band, leaving holes in the valence band. The number of electron-hole pairs is proportional to the number of the absorbed photons and thus to the light power  $P_L$  (or, respectively, the light intensity  $I_L$ ) of the incident light.

The creation of electron-hole pairs occurs in the p-region, the n-region and in the depletion zone of the photodiode. The charge carriers generated in the depletion zone can directly be separated spatially and accelerated by the existing electric field  $E$  (Fig. 11). Charge carriers that were generated in the p- and n-layers must reach the depletion layer by diffusion prior to recombination, before they can be accelerated there.

If the contacts of the p- and n-layer are connected (Fig. 12 left and centre), a photocurrent  $I$  flows, consisting of a *drift current* (photon absorption in the depletion layer) and a *diffusion current* (photon absorption outside the depletion layer) which changes in linear proportion to the incident light power  $P_L$  or intensity  $I_L$ , respectively. This is the simplest mode of operation of a photodiode<sup>12</sup>.

<sup>12</sup> In this mode of operation, we often speak of a *photoelement* instead of a *photodiode*.



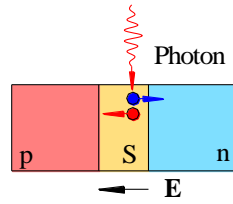


Fig. 11: Creation of an electron-hole pair, here by absorption of a photon in the depletion zone S of a photodiode. The charge carriers (electron and hole) are separated and accelerated by the electrical field  $E$ .

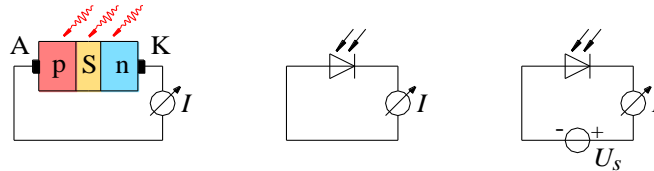


Fig. 12: *Left*: Schematic representation of a pn-photodiode irradiated by light causing a photocurrent  $I$ . Black: Contacts of the p-layer (anode A) and the n-layer (cathode K). *Centre*: Associated circuit diagram. The vertical bar in the diode symbol symbolizes the cathode K. *Right*: Circuit diagram of a photodiode with reverse voltage  $U_s$ .

Photodiodes are often operated with an externally applied *reverse voltage*  $U_s$  between anode and cathode (cf. Fig. 12 right).  $U_s$  is usually in the range of several volts. Thereby the width of the *barrier layer* S increases. This lowers its capacitance  $C$  (analogue to  $\rightarrow$  *parallel plate capacitor*). Furthermore,  $U_s$  causes an increase of the electrical field strength  $E$  within the barrier layer, thereby accelerating the charge carriers more strongly. Both effects combined cause a reduction of the time constant  $\tau = RC^{13}$  of the output signal of the photodiode down to the 10 ns range. In this way, it becomes possible to measure rapid changes in incident light power (or light intensity).

### 2.5.3 Technical Realization of a Photodiode

In order to produce a photodiode one starts out according to Fig. 13 (left) with a piece *n-type-Si* (*bulk material*) being several (10 – 100)  $\mu\text{m}$  thick. Next, a mask of  $\text{SiO}_2$  is applied to the material. This mask limits the light sensitive area of the photodiode to the area not covered by  $\text{SiO}_2$ . Subsequently, three valenced atoms are introduced into the bulk material by diffusion or ion-implantation, until in a thin layer (thickness in the range of 1  $\mu\text{m}$ ), the p-layer, a surplus of p-charge carriers has been established by the doping process. A thin barrier layer S (thickness also in the  $\mu\text{m}$  range) establishes itself between this layer and the n-material. The final step is to add metallic contacts to the p- and n-layers (cf. Fig. 13 left and right) and, if needed, apply an anti-reflective layer (AR). The finished diode is usually closed in by a protective glass (G).

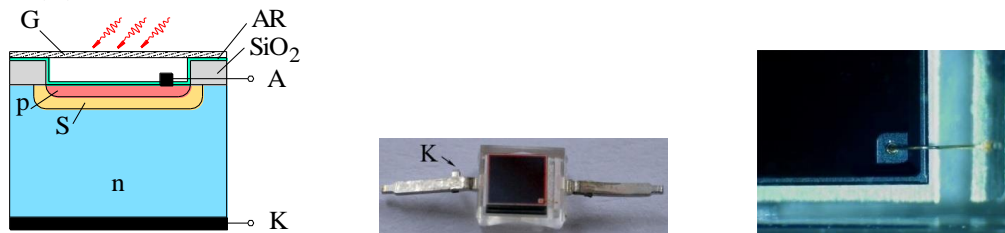


Fig. 13: *Left*: Schematic representation of the cross-section of a Si-photodiode. The anti-reflective layer (AR) is drawn in green colour, while the metallic contacts are colored black. G is a protective glass. *Centre*: Photograph of a photodiode (SIEMENS BPW 34) with soldering contacts bent to the side. The anode contact A, which is connected to the soldering contact on the right hand side, is located at the lower right of the black, light-sensitive plane. The lug on the left soldering contact serves to mark this contact as the connecting contact of the cathode K. *Right*: Enlarged cutout of the front side of the photodiode under a microscope. The anode contact, which is about  $0.25 \times 0.25 \text{ mm}^2$  in size and has a gold connecting wire (bond wire) with a diameter of about 25  $\mu\text{m}$  can be seen on the bottom right of the black, light-sensitive plane. The wire is connected to the anode's soldering contact on the right. The outer border and parts of the gold wire appear blurred because the focus was set on the plane of the anode-contact.

<sup>13</sup>  $R$  is the decisive resistance for the time constant in the external wiring of the photodiode.

The *spectral sensitivity*  $S_\lambda$  of a photodiode at the wavelength  $\lambda$  is defined as the quotient of photocurrent  $I$  and light power  $P_L$  of the irradiation:

$$(8) \quad S_\lambda = \frac{I}{P_L} \quad \text{with} \quad [S_\lambda] = \text{A/W}$$

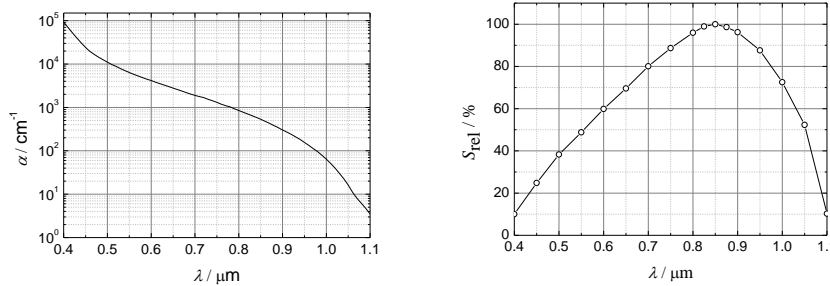


Fig. 14: *Left:* Absorption coefficient  $\alpha$  of silicon as a function of the wavelength  $\lambda$  (Data source: A. M. GREEN, Solar Energy Materials & Solar Cells 92 (2008) 1305–1310).  
*Right:* Relative spectral sensitivity  $S_{\text{rel}}$  of the photodiode Siemens BPW 34 as a function of the wavelength  $\lambda$ . (Data source: SIEMENS-Datasheet.)

The larger the wavelength  $\lambda$  of the light, by which the photodiode is illuminated, the smaller the absorption coefficient  $\alpha$  (Fig. 14 left) and the larger therefore the penetration depth of the photons. Short-wave light is largely absorbed by the protective glass, the anti-reflective layer, or the p-layer, while long-wave light is (mostly) not absorbed before reaching the n-layer. The further away from the depletion layer the photo absorption takes place, the smaller the probability that charge carriers can diffuse to the depletion layer before they recombine. Therefore such photons can only contribute little to the photocurrent. Thus, in total, the photodiode has a  $\lambda$ -dependent spectral sensitivity with an upper limit depending on the band-gap of the semiconductor material (about 1.1  $\mu\text{m}$  for Si). As an example, Fig. 14 (right) shows the *relative* spectral sensitivity  $S_{\text{rel}}(\lambda)$  of the photodiode used in the laboratory course.

### 3 Experimental Procedure

#### Attention:

*Special care must be taken to avoid direct or indirect (by reflection) exposure of the eyes to the laser beam, when conducting experiments involving lasers. Severe retina damage may be caused by the extremely high light intensities! The laser beam must therefore be kept below a height of 1.2 m at all times!*

#### Equipment:

Digital oscilloscope TEKTRONIX TDS 1012 / 1012B / 2012C / TBS 1102B - EDU, digital multimeter (AGILENT U1251B, FLUKE 112 and MATRALINE DM 62), 3 power supplies (PHYWE 0 - 15 / 0 - 30 V), force sensor (U-OL) with measuring amplifier (U-OL), set of weights, aluminum-ring, laboratory balance, pressure sensor (SENSORTECHNICS HCLA12X5DB) on base plate with gate valves on mount, ERLNMEYER flask with ground in glass stopper on table, U-pipe-manometer (water filling) with mount and scale, beaker glass on support jack, tubing, laser distance sensor (BAUMER OADM 12U6460/S35), spring with bar and ball on mount, beaker glass with glycerin/water-mixture (190 ml water on 1000 ml glycerine), base plate with angle sensor (TWK-ELEKTRONIK PBA 12) and hand-wheel, photodiode SIEMENS BPW 34, grid-style printed circuit board ( $8 \times 5 \text{ cm}^2$ ) for mounting the photodiode with accessories (50  $\Omega$ -resistor, cable, insulating tape, solder), soldering station, wire stripper, clamps, helium-neon laser on triangular rail, polarization filter in THORLABS rotatable mount, U-mount for photodiode, slider.

#### Note:

Selected characteristics of the sensors used are listed in Tab. 1 of the appendix (Chap. 4).

#### 3.1 Calibration of a Force Sensor

The force sensor suspended from a mount is to be calibrated with the aid of a set of weights. For this purpose, the force sensor is connected to the measuring amplifier, which amplifies the bridge voltage  $U$  to the voltage  $U_M$ . The measuring amplifier draws its operating voltage from a power supply, the Damping (Dämpfung) is switched on. The output voltage of the measuring amplifier is measured with a voltmeter for at least 5 weights  $G$  in the range of (0 - 100) mN. For the calculation of the masses  $m$  of the weights from  $G = mg$ , the value of the gravitational acceleration in Oldenburg,  $g = 9.8133 \text{ m/s}^2$  is used, which is



as well as  $m$  assumed to be an error free quantity<sup>14</sup>. Subsequently,  $G$  is plotted over the measured values of  $U_M$  and a calibration curve is determined. Since the sensor operates linear, the calibration curve is a line; its parameters are determined by performing a linear regression.

Finally, an unknown test object is attached to the force sensor, and the output voltage  $U_M$  of the measuring amplifier is recorded. With the aid of the calibration curve, the weight  $G$  and the mass  $m$  of the object are determined. The maximum error of  $m$  follows from the maximum error of  $U_M$ , the errors of the parameters of the regression line may be neglected. In addition,  $m$  is also measured by a laboratory balance (error negligible). Both measured values are compared.

### 3.2 Calibration of a Pressure Sensor

The pressure sensor is calibrated by applying defined pressure differences  $\Delta p$  between both of its tube connectors and measuring the resulting output voltage  $U$  for each case.

The tube connector labeled “-“ is left open, thus remaining in direct contact with the surrounding atmosphere. The connector labeled “+“ is connected to the volume of gas, for which the *overpressure*  $\Delta p$  relative to the surrounding is to be measured. Operating the sensor in this mode requires  $\Delta p \geq 0$  in order to obtain a linear response from the sensor (i.e. the pressure at the “+“-connector must be greater than the pressure at the “-“-connector). The maximum allowed pressure difference is  $\Delta p = + 1.25 \times 10^3$  Pa, which is converted to a voltage signal of  $U = U_0 + 2$  V ( $U_0 = 2.25$  V)<sup>15</sup> for a supply voltage of + 5 V (power supply). The pressure difference  $\Delta p = 0$  Pa creates a voltage of  $U = U_0 + 0$  V =  $U_0$ . For pressure differences in the interval between 0 Pa and  $1.25 \times 10^3$  Pa, the output voltages lie in the interval  $U_0 \leq U \leq U_0 + 2$  V<sup>16</sup>.

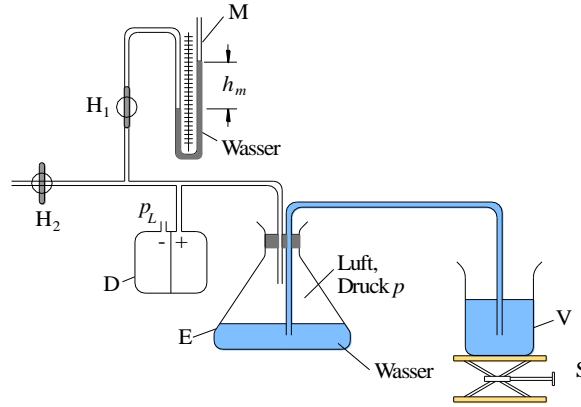


Fig. 15: Setup for creating pressure differences  $\Delta p > 0$  relative to the ambient pressure  $p_L$ . For details, refer to the text.

The pressure differences required for the calibration of the sensor can be established by using a setup according to Fig. 15. The volume of air in an airtight ERLLENMEYER flask E is connected to the pressure sensor D and an U-pipe manometer M by a system of tubes (valve  $H_1$  open, valve  $H_2$  closed). The pressure  $p$  in this volume may be changed by variation of the water level in E. This variation is achieved through raising and lowering a water filled storage vessel (beaker glass) V by using the support jack S. V and E are connected by a hose dipping into the water in both containers. The difference between the pressure  $p$  in E and the ambient pressure  $p_L$ ,

$$(9) \quad \Delta p = p - p_L$$

can be measured with the U-pipe manometer. For a difference in height  $h_m$  in the manometer, it is given by:

$$(10) \quad \Delta p = \rho_m h_m g$$

<sup>14</sup> Value taken from <http://www.ptb.de/cartoweb3/SISproject.php> (01.09.2015); the error of  $2 \times 10^{-5}$  m/s<sup>2</sup> is neglected.

<sup>15</sup> Note that it would be possible to operate the sensor by keeping the “+“-connector in contact with the surrounding and connecting a volume of gas at a negative pressure to the “-“-connector. The maximum pressure difference would be  $\Delta p = - 1.25 \times 10^3$  Pa, which would be converted to a voltage signal of  $U = U_0 - 2$  V.

<sup>16</sup>  $U_0$  and  $U$  vary with the operating voltage (nominal 5 V). An once adjusted voltage may not be changed therefore during the measuring.

where  $\rho_m$  is the density of the liquid in the manometer (here: water) and  $g$  the gravitational acceleration of earth ( $g$  as in Chap. 3.1). A value of  $998 \text{ kg/m}^3$  may be used for the density  $\rho_m$  of water in the temperature range  $(20 \pm 2) \text{ }^\circ\text{C}$  and considered to be exact.

**Question 1:**

What is the maximum value for the height  $h_m$  that may be used without exceeding the maximum pressure difference of the sensor?

The output voltage  $U$  of the pressure sensor D is measured with a voltmeter for at least 5 different pressure differences (measure the associated heights  $h_m$ ).  $\Delta p$  (Eq. (10)) is plotted over  $U$ . Error bars for  $\Delta p$  are drawn which arise from the maximum errors of the heights  $h_m$ . After all, the calibration curve is determined and drawn. Since the sensor operates linearly, the calibration curve is a line; its parameters are obtained by using the method of linear regression.

**Note about the noise:**

The electronic noise of the pressure sensor (cf. Tab. 1 in the appendix, Chap. 4) causes fluctuations of the output voltage  $U$ , which can be converted into noise of the pressure signal by using the calibration function. This noise is smaller than the pressure fluctuations according to Eq. (10), which are caused by the limited accuracy in reading off the height difference  $h_m$ . Thus, it may be neglected for the measurements to be performed here.

### 3.3 Distance Measurement with a Laser Distance Sensor

The temporal behavior of a damped harmonic oscillation is to be investigated by employing a laser distance sensor (type BAUMER OADM 12U6460/S35). The angular frequency  $\omega$  of the oscillation and the damping constant  $\alpha$  are sought-after. To measure both quantities we proceed as follows:

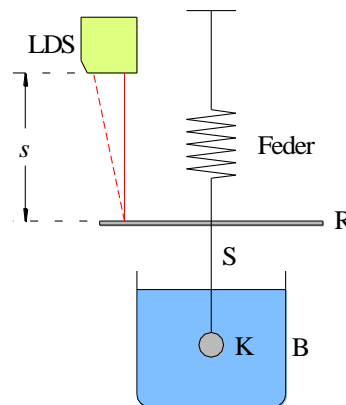


Fig. 16: Measuring the course of a damped harmonic oscillation using a laser distance sensor LDS.

A ball  $K$  is connected to a spring by a rod  $S$  according to Fig. 16. The ball is dipped in a glass beaker  $B$  containing a glycerin/water mixture providing a damping of the motion. The rod  $S$  is released after displacing it downwards by several centimeters (adhere to the measuring range of the sensor, cf. Table 1 in the appendix). This causes the ball and bar to execute a damped harmonic oscillation. The displacement from the initial position,  $x$ , can be described as a function of the time  $t$  by the following equation:

$$(11) \quad x(t) = x_0 e^{-\alpha t} \cos(\omega t)$$

where  $x_0$  is the initial amplitude (i.e. the initial displacement of the ball),  $\omega$  the angular frequency of the oscillation, and  $\alpha$  the damping constant. Let  $t = 0$  be the time when the bar is released.

The displacement  $x(t)$  is converted into a voltage signal  $U(t)$  by the laser distance sensor. For this purpose, the bar  $S$  is fitted with a reflective disk  $R$  at which the laser beam of the sensor is aimed. The output voltage of the sensor is given by:

$$(12) \quad U(t) = U_0 e^{-\alpha t} \cos(\omega t) + U_{DC}$$

Here  $U_{DC}$  is a direct voltage part depending on the distance between the laser distance sensor LDS and the reflector disc R in the zero position of the sphere.

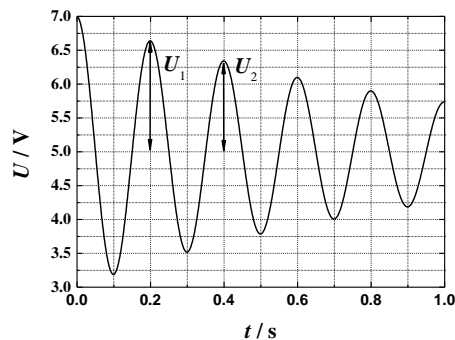


Fig. 17: Exemplary representation of the output signal of the laser distance sensor according to Eq. (12). In this example  $U_0 = 2 \text{ V}$  and  $U_{DC} = 5 \text{ V}$ . The voltages  $U_i$  are measured at the instants  $t_i$  (here  $t_0 = 0 \text{ s}$ ,  $t_1 = 0.2 \text{ s}$ ,  $t_2 = 0.4 \text{ s}, \dots$ ).

$U(t)$  is recorded with a digital storage oscilloscope in the **SINGLE-SEQ**-mode. From the recorded curve the frequency  $f$  of the damped oscillation is measured with the time cursors and from that  $\omega$  is calculated. In order to determine the damping constant  $\alpha$ , the amplitudes  $U_i$  of the partial oscillations at the instants  $t_i$  ( $i = 0, 1, 2, \dots$ ) are measured with the voltage cursors (Fig. 17). No errors must be indicated for  $U_i$  and  $t_i$ .  $U_i$  is plotted vs.  $t_i$  in a semilogarithmic diagram ( $U_i$  on a logarithmic axis). If the natural logarithm is used for scaling the ordinate, then  $\alpha$  results from the slope of the regression line through the measured values.<sup>17</sup>

It is possible to convert the voltage signal  $U(t)$  to the quantity  $x(t)$  by calibrating the sensor.

### Question 2:

How would one proceed in order to produce a calibration curve?

Since the relationship between  $U(t)$  and  $x(t)$  is linear, both functions would exhibit the same form. For this reason, calibration and conversion are to be neglected in this case.

### Question 3:

How could the velocity  $v(t)$  and the acceleration  $a(t)$  be obtained from the course of  $x(t)$ ? What does the graph  $x(t)$  look like?

## 3.4 Measurement of a Transmission Ratio with an Angle Sensor

A hand-wheel H and an angle sensor W are mounted on a base plate according to Fig. 18. A disk with an O-ring pushing against the rim of the hand-wheel is mounted on the rotational axis of the angle sensor. The output voltage  $U_W$  of the angle sensor changes in a linear manner between  $U_{min}$  (approx. 0 V) and  $U_{max}$  (approx. 5 V) for a full rotation of its axis.

The hand-wheel is turned once from  $\beta = 0^\circ$  to  $\beta = 360^\circ$  (that is by  $2\pi$ ). Thereby W turns by the angle  $\alpha > 2\pi$ . The transmission ratio  $V = \alpha/2\pi$  between the rotation of W and the hand-wheel is determined by measurement of  $U_{min}$ ,  $U_{max}$ ,  $U_{\beta=0^\circ}$ ,  $U_{\beta=360^\circ}$  with a voltmeter and the number  $n$  of voltage-jumps from  $U_{max}$  to  $U_{min}$  that occur while  $\beta$  is modified. A statement of the error of  $V$  is not required.

<sup>17</sup> Take into account the hints to the linear regression in (semi-)logarithmic diagrams in the chapter „Usage of Computers...“ („Apparent fit“).

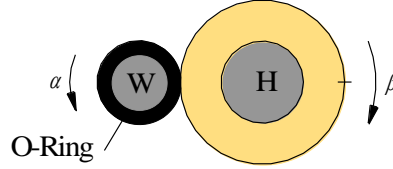


Fig. 18: Angle sensor W with O-ring pushing against the rim of a hand-wheel H. Rotation of the hand-wheel by the angle  $\beta$  causes the O-ring and thus the axis of W to rotate by the angle  $\alpha$ .

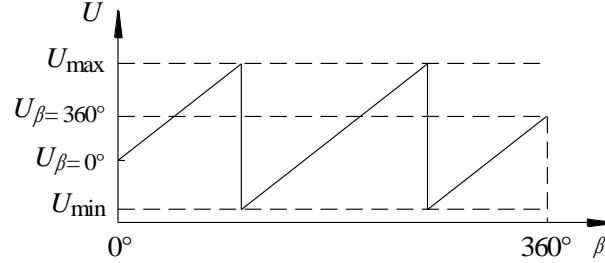


Fig. 19: Output voltage of the angle sensor during rotation of the hand-wheel H (Fig. 18) by  $\beta = 360^\circ$  (exemplary!). In the hand-wheel position  $\beta = 0^\circ$  the axis of the angle sensor is at an arbitrary angle position, at which the output voltage of the angle sensor is  $U_{\beta=0^\circ}$ .

### 3.5 Measurements with a Photodiode

#### 3.5.1 Linearity of the Output Signal of a Photodiode

The aim of the measurement is the validation of the linear relationship between the photocurrent of a photodiode and the incident light power.

The photodiode of the type Siemens BPW 34<sup>18</sup> (Fig. 13) is soldered to the upper end of the circuit board. Connection cables with tinned ends are produced for the anode and cathode and are soldered to the diode. Clamps are attached to the free ends of the cables in order to connect the photodiode to an ammeter (AGILENT U1251B) through laboratory cables. The lower end of the circuit board is wrapped with insulating tape and fixed on an U-mount.

Validation of the linearity of the photodiode mandates exposing it to light of varying intensities  $I_L$ . Varying intensities of light are easily produced by using a combination of laser and an *ideal* polarization filter. We employ a helium-neon laser ( $\lambda \approx 633$  nm) emitting linearly polarized light (i.e. the electrical field  $\mathbf{E}$  of the light wave oscillates in only one direction). This light is passed through a rotatable polarization filter with the property of permitting only one direction of the  $\mathbf{E}$ -field to pass through. If  $\mathbf{P}$  is the permissive direction of the polarization filter,  $\mathbf{E}$  the direction of the electric field of the light wave incident to the filter and  $\alpha$  the angle between  $\mathbf{E}$  and  $\mathbf{P}$ , then only the component  $\mathbf{E}_t$  of  $\mathbf{E}$  which is parallel to  $\mathbf{P}$  is transmitted. According to Fig. 20 this component is:

$$(13) \quad \mathbf{E}_t = \mathbf{E} \cos \alpha$$

The intensity of a light wave is determined up to a proportionality factor  $k$  by the square of its amplitude  $E = |\mathbf{E}|$ . If the intensity of the laser light is  $I_L$ , it follows from Eq. (13) that the intensity transmitted through the polarization filter,  $I_p$ , is given by MALUS<sup>19</sup> law:

$$(14) \quad I_p = k E_t^2 = k E^2 \cos^2(\alpha) = I_L \cos^2(\alpha)$$

Thus, varying light intensities  $I_p$  may be achieved simply by rotating the polarization filter by an angle  $\alpha$ .

<sup>18</sup> BPW 34 is a PIN-photodiode differing slightly in its construction from the pn-photodiode described in this text. The details of the differences between both types are not covered here, since they are irrelevant for the experiments conducted in this laboratory session.

<sup>19</sup> ETIENNE LOUIS MALUS (1775–1812). The measurable absorption of the polarization filter for the case  $\mathbf{E} \parallel \mathbf{P}$  is neglected here.

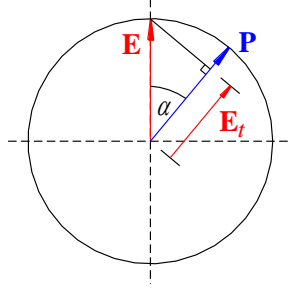


Fig. 20: Transmission of a linearly polarized light wave with the electrical field vector  $\mathbf{E}$  through a polarization filter with permissive direction  $\mathbf{P}$ .

The laser is mounted on the triangular rail, followed by the polarization filter  $\mathbf{P}$ , and finally the photodiode  $\text{FD}$ . The photodiode is aligned so that the laser beam is incident on its centre.

First, the orientation of  $\mathbf{E}$  of the light wave emitted by the laser must be determined. For this purpose, the current  $I$  of the photodiode is measured while varying the angular setting of the polarization filter  $\mathbf{P}$ .  $I$  is minimal, if  $\mathbf{E}$  and  $\mathbf{P}$  are orthogonal. In this position,  $\alpha = 90^\circ$  and the value  $\beta$  is shown on the angle scale of the polarization filter. Since the orientation of the laser in its mount can be arbitrary,  $\beta \neq \alpha$  in general.

Subsequently, the shutter of the laser is closed and the dark current  $I_D$  of the photodiode is measured. Next, the shutter is reopened and the photocurrent  $I$  is measured for varying angles  $\alpha$  ( $\alpha = (0, 10, 20, \dots, 90)^\circ$ ), which can be set with the help of the angular scale on the polarization filter. The current difference

$$(15) \quad I_\alpha = I - I_D$$

is proportional to the light intensity  $I_p$ .  $I_\alpha$  is plotted over  $\cos^2(\alpha)$  and a linear regression is carried out to obtain a linear best fit. The linearity of the photodiode can be judged by looking at the distribution of the measured values in relation to the regression line. Random deviations of the measured values from the regression line are explained by the *real* properties of the polarization filter, systematic deviations would indicate a nonlinear behaviour of the photodiode.

### 3.5.2 Measuring the Power of Laser Light

The spectral sensitivity  $S_\lambda$  of the photodiode used (BPW 34) at the wavelength  $\lambda = 850 \text{ nm}$  can be found in the data sheet:  $S_{850 \text{ nm}} = 0.62 \text{ A/W}$  (without any stated error). Knowledge of the relative spectral sensitivity  $S_{rel}$  for  $\lambda = 633 \text{ nm}$  provided (cf. Fig. 14 right), it is possible to deduce the spectral sensitivity  $S_\lambda$  for the wavelength of the laser light ( $\lambda \approx 633 \text{ nm}$ ):

$$(16) \quad S_{633 \text{ nm}} = S_{850 \text{ nm}} \frac{S_{rel}(633 \text{ nm})}{100} \quad S_{rel} \text{ in } \%$$

The polarization filter is removed from the setup for measuring the power of the laser light  $P_L$  in order to irradiate the photodiode directly and the photocurrent  $I_{633 \text{ nm}}$  is measured. Once  $I$  has been measured, the shutter of the laser is closed and the dark current  $I_D$  of the photodiode is measured. The difference  $I = I_{633 \text{ nm}} - I_D$  is the net current needed for the determination of the light power  $P_L$  according to Eq. (8). For the calculation of the error of  $P_L$  only the reading error of  $S_{rel}$  is to be taken into account. In addition to the measured value the number of the used laser is indicated.

### 3.5.3 Measuring the Speed of Finger Movement

The following experiment measures how fast a stretched, horizontally oriented finger can be moved about  $(30 - 40)^\circ$  downwards – a virtuous piano player will certainly be faster at this than other people. This is done by holding the fingertip just above the laser beam, and subsequently moving the finger (not the hand) downwards as fast as possible. The laser beam is thus blocked off for a moment by the intersecting fingertip. The (time) period of intersection is measured with the photodiode and shall serve as a measure of speed. The influence of finger thickness is neglected.

The measurement is to be done using a digital storage oscilloscope operated in the **SINGLE-SEQ**-mode. A requirement for this is the transformation of the photocurrent  $I$  into a voltage  $U$ . The easiest way to achieve this is to let  $I$  flow through a resistor  $R$  and measuring the voltage drop over the resistor using  $U = RI$ <sup>20</sup>. Additionally, in order to reduce the time constant, the photodiode must be operated with a reverse voltage  $U_S$  (cf. Chap. 2.5.2). This is the prerequisite for the measurement of rapid changes in light intensity. Fig. 21 shows the associated circuit diagram.

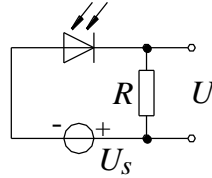


Fig. 21: Circuit configuration for a photodiode for measuring rapid changes in light intensity  $I_L$  as a function of time  $t$ . The temporal course of the voltage,  $U(t) \sim I_L(t)$ , may be recorded by a digital storage oscilloscope.

To create the setup according to Fig. 21, the resistor  $R \approx 50 \Omega$  is soldered to the circuit board and fitted with a connecting cable (in addition to the photodiode). The block voltage should be  $U_S = 10 \text{ V}$ . Once this has been completed, the measurement is carried out for the index finger and the ring finger of the right- and left hand.

#### Question 4:

Are there any significant differences in the results by comparing the index finger with the ring finger as well as right- with the left hand? Describe and discuss your experimental results.

## 4 Appendix

Tab. 1: Selected characteristics of the used sensors as far as available or possible to indicate.

Quantity	Type	Measuring range	Resolution	Response time	Noise
Force	U-OL 227/10	(0 – 100) mN		< 0.5 ms	$\pm 0.7 \text{ mV}$
Pressure	SENORTECHNICS HCLA 12X5DB	(0 – 1250) Pa		0.5 ms	$\pm 4 \text{ mV}$
Distance	BAUMER OADM 12U6460/S35	(16 – 120) mm	(0.002 – 0.12) mm <sup>21</sup>	< 0.9 ms	$< \pm 5 \text{ mV}$
Angle	TWK-ELEKTRONIK PBA 12	(0 – 360)°	0.35°	< 0.4 ms	< 0.5°
Light power	SIEMENS BPW 34			20 ns <sup>22</sup>	NEP <sup>23</sup> $4.1 \times 10^{-14} \text{ W/Hz}^{-1/2}$

<sup>20</sup> In advanced measurement technology *transimpedance amplifiers* based on operational amplifiers are used for current/voltage conversion. The required components are discussed in part II of the introductory laboratory course.

<sup>21</sup> The smaller the distance between the LDS and the object under measurement, the better the resolution.

<sup>22</sup> Depending on circuit set-up.

<sup>23</sup> NEP: *noise equivalent power*.